Asymmetry in ENSO Teleconnection with Regional Rainfall, Its Multidecadal Variability, and Impact

Wenju Cai, Peter van Rensch, Tim Cowan, and Arnold Sullivan

CSIRO Marine and Atmospheric Research, Aspendale, Victoria, Australia

ABSTRACT

An asymmetry, and its multidecadal variability, in a rainfall teleconnection with the El Niño–Southern Oscillation (ENSO) are described. Further, the breakdown of this relationship since 1980 is offered as a cause for a rainfall reduction in an ENSO-affected region, southeast Queensland (SEQ). There, austral summer rainfall has been declining since around the 1980s, but the associated process is not understood.

It is demonstrated that the rainfall reduction is not simulated by the majority of current climate models forced with anthropogenic forcing factors. Examination shows that ENSO is a rainfall-generating mechanism for the region because of an asymmetry in its impact: the La Niña–rainfall relationship is statistically significant, as SEQ summer rainfall increases with La Niña amplitude; by contrast, the El Niño–induced rainfall reductions do not have a statistically significant relationship with El Niño amplitude. Since 1980, this asymmetry no longer operates, and La Niña events no longer induce a rainfall increase, leading to the observed SEQ rainfall reduction. A similar asymmetric rainfall teleconnection with ENSO Modoki exists and shares the same temporal evolutions.

This breakdown is caused by an eastward shift in the Walker circulation and the convection center near Australia's east coast, in association with a post-1980 positive phase of the interdecadal Pacific oscillation (IPO). Such a breakdown occurred before 1950, indicating that multidecadal variability alone could potentially be responsible for the recent SEQ rainfall decline. An aggregation of outputs from climate models to distill the impact of climate change suggests that the asymmetry and the breakdown may not be generated by climate change, although most models do not perform well in simulating the ENSO–rainfall teleconnection over the SEQ region.

1. Introduction

The El Niño–Southern Oscillation (ENSO) cycle is the dominant mode of climate variability affecting many parts of the globe including eastern Australia, where it is widely accepted that El Niño events increase the risk of drought, whereas La Niña years are associated with floods (McBride and Nicholls 1983; Ropelewski and Halpert 1987; Philander 1990). The affected Australian regions include southeast Queensland (SEQ; encompassing 20.5°–30.5°S, 150.5°–154.5°E, covering an area of approximately 210 000 km², denoted by a border in Fig. 1), where austral summer [December–February (DJF)] rainfall accounts for most of the annual total. Over recent decades, there has been a decline in summer rainfall, as a result of a reduction in heavy rainfall events with much lower monthly totals since 1980 (Fig. 1b), contributing to about a 20% reduction since 1950, amid significant reductions over other Australian regions (Fig. 1a, Cai et al. 2001; Alexander et al. 2007). This observed reduction can also be viewed as a significant linear step jump (at the 99% confidence level) around 1975 using breakpoint analysis (figure not shown), consistent with the shift in the interdecadal Pacific oscillation (IPO) during this time (Meehl et al. 2009).

Numerous studies have examined similar declines over southwest Western Australia (e.g., Smith et al. 2000; Cai et al. 2005; Hope et al. 2006; Cai and Cowan 2006), and across southeast Australia (Cai and Cowan 2008), but few have focused on the reduction over SEQ. In one such study, Syktus (2005) shows that incorporating a stratospheric ozone depletion forcing to climate model simulations appears to contribute to a drying trend in annual rainfall across eastern Australia from 1993–2003. This is as a result of changes in Southern Hemisphere mean sea level pressure, related to a positive trend in the southern

Corresponding author address: Wenju Cai, CSIRO Marine and Atmospheric Research, PMB 1, Aspendale, VIC 3195, Australia.
E-mail: wenju.cai@csiro.au

(a) Summer rainfall trends 1950-2008
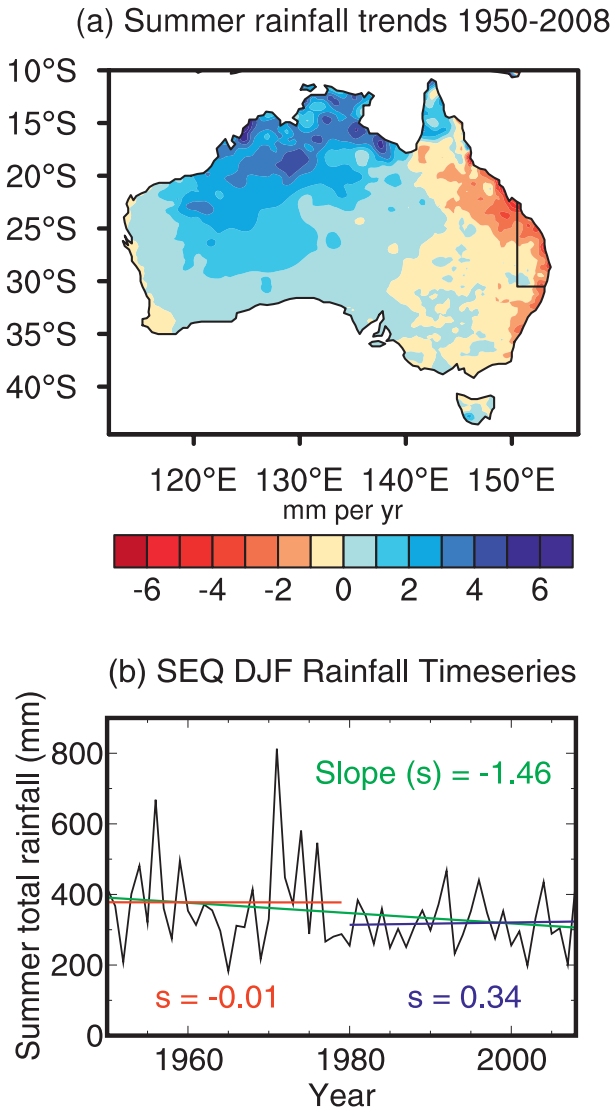

(b) SEQ DJF Rainfall Timeseries

FIG. 1. (a) Australian DJF rainfall trends over the period 1950–2008 (mm year^{-1}). The bordered area indicates the SEQ region. (b) SEQ summer rainfall time series together with trend lines over 1950–79 (red), 1980–2008 (blue), and 1950–2008 (green). The spatial trend pattern and time series are taken from interpolated homogeneous station data, provided by the Australian Bureau of Meteorology (see section 2).

annular mode in austral summer. However, the seasonality of this ozone depletion linkage with SEQ rainfall has not been investigated using multimodel outputs. Cai et al. (2001) suggest that the decline is consistent with an El Niño–like warming pattern in response to global warming, as simulated by a climate model (Meehl and Washington 1996). This type of an El Niño–like rainfall response is now in question (Collins 2005; Vecchi et al. 2006), although the associated eastward shift and a weakening of the climatological Walker circulation are

simulated by most models used for the Intergovernmental Panel on Climate Change (IPCC) Fourth Assessment Report (AR4). On the other hand, SEQ summer rainfall is a part of an Australia-wide annual total rainfall influenced by the multidecadal variability of ENSO (Power et al. 1999). Furthermore, a nonlinear relationship exists between ENSO and Australian rainfall during the peak ENSO impact months (June–December), whereby strong La Niña events have been linked to a large continental rainfall response, whereas El Niño events are more unreliable in terms of their impact (Power et al. 2006). However, the robustness and the mechanism of such an asymmetric teleconnection have not been addressed. Here, we show that significant multidecadal fluctuations exist in the asymmetry. We then examine the mechanism and demonstrate that a collapse of the asymmetry since 1980, with La Niña no longer inducing a higher rainfall, is a process leading to the recent SEQ summer rainfall reduction. We address whether the reduction and the associated processes are captured by the IPCC AR4 twentieth-century climate model experiments and whether anthropogenic climate change plays a part.

Another issue is whether the observed reduction is induced by a different ENSO pattern, referred to as ENSO Modoki (Ashok et al. 2007), which has the anomaly center at the date line rather than in the central eastern Pacific and has occurred more frequently in recent decades. During an El Niño Modoki event, there are two anomalous Walker circulation cells in the troposphere, instead of the single-celled pattern of the conventional El Niño. The core rising branch of the double-celled Walker circulation is located over the central equatorial Pacific, and the associated western-descending branch is situated over Indonesia and northern Australia; therefore, it is more effective in suppressing Australian rainfall. In spring, this explains the inter-event difference of the impact on Australia rainfall between the 2002 El Niño (a dominantly Modoki event, with extremely dry conditions across Australia) and the 1997 episode (conventional El Niño, with little rainfall reduction in Australia; Wang and Hendon 2007). However, the situation in autumn is different in that only La Niña Modoki events have a statistically significant impact over Australia (Cai and Cowan 2009). The influence in summer is not well understood. We therefore explore whether climate models can first simulate the long-term SEQ summer rainfall changes (section 3), and second, how much of this change is due to the asymmetric teleconnection of ENSO and ENSO Modoki with rainfall (sections 4 and 5). The issue of multidecadal variability as a catalyst for the SEQ rainfall reduction is highlighted in section 6.

2. Model experiments, reanalysis, and observations

We analyze the twentieth-century experiments from 24 models submitted as part of the IPCC AR4, comprising a total of 75 simulations made available through the third Coupled Model Intercomparison Project (CMIP3). Model names and details are listed in Table 1 of Cai et al. (2009) with references to further documentation. Two-thirds of models have multiple ensemble members. A total of 44 experiments include a stratospheric ozone forcing component, whereas the rest do not, allowing stratification into two groups: with and without ozone depletion. Because ozone forcing may not be the only difference between these two groups, and as all models include an anthropogenic aerosol forcing in one form or another, we have also analyzed a series of targeted multimember ensemble experiments with the Commonwealth Scientific and Industrial Research Organisation Mark 3A (CSIRO Mk3A) model (Rotstayn et al. 2007), which is designed to isolate the impacts of individual forcing factors. The impact of ozone depletion (four ensemble members) and greenhouse gases only (four ensemble members) in these targeted Mk3A experiments are realized by forcing the model with a time-evolving forcing alone, whereas the impact of an anthropogenic aerosol forcing is obtained by comparing two sets of experiments (eight ensemble members each) with and without increasing aerosols, both in the presence of all other forcing factors.

As will be shown (section 3), the majority of models and targeted model experiments do not simulate the observed rainfall reduction since 1950. If these models are perfect, it would imply that multidecadal variability plays a role in forcing the observed reduction. Given that ENSO is the dominant driver of rainfall variability across eastern Australia, we examine whether the changing properties, the associated multidecadal-mean state in the Pacific (Wang 1995), and ENSO Modoki plays a part in the observed reduction. To this end, an updated version of the Hadley Centre's Global Sea Ice and Sea Surface Temperature (SST) reanalysis (Rayner et al. 2003), covering data since 1870, is used to construct a Niño-3.4 index (5°S–5°N, 170°–120°W), ENSO Modoki index (EMI), and their associated circulation patterns. The EMI is defined as $EMI = [SSTA]_A - 0.5 \times \{[SSTA]_B + [SSTA]_C\}$, where the square brackets represent the area-averaged SST anomalies for the regions A (10°S–10°N, 165°E–140°W), B (15°S–5°N, 110°–70°W), and C (10°S–20°N, 125°–145°E), respectively (Ashok et al. 2007).

As a means of providing information for the latter sections, Fig. 2 displays the anomaly pattern associated with ENSO and the ENSO Modoki through a regression of SST onto their respective indices (e.g., Niño-3.4 and
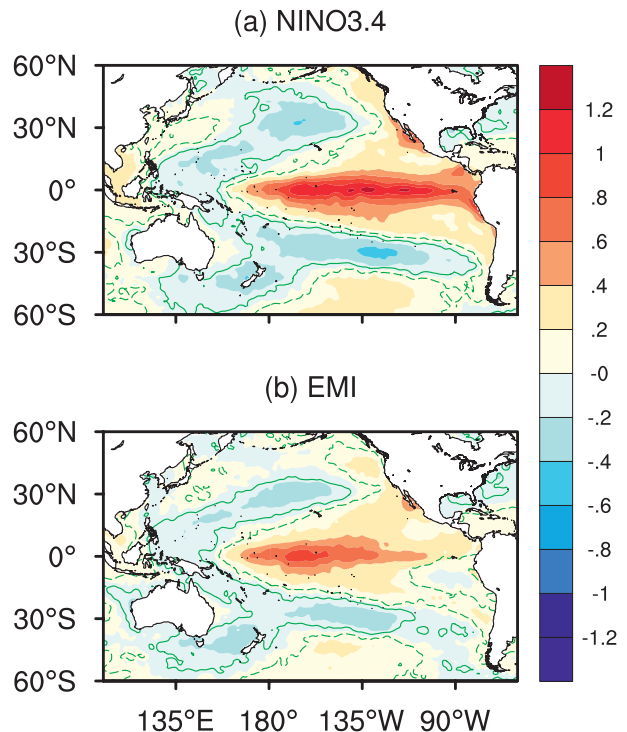

FIG. 2. One standard deviation anomaly pattern obtained by linearly regressing observed gridpoint SST onto (a) detrended Niño-3.4 and (b) detrended EMI, and then multiplying by the one standard deviation value of the index. Dashed (solid) green contours indicate positive (negative) correlations significant at the 90% confidence level. Patterns shown are for DJF.

EMI). Austral summer is the season in which traditional ENSO and ENSO Modoki events peak, while SST anomalies associated with both types are similar, well developed, and occupy almost the entire equatorial Pacific. Indeed the correlation between the EMI and Niño-3.4 (both detrended) for this season using samples since 1950 is rather high, at 0.65. In other seasons (e.g., austral spring and autumn), the EMI displays a warm SST anomaly in the date line region but cool anomalies to the east and the west. In the case of summer, the cooling in the eastern Pacific is weak (Fig. 2b), suggesting that there is no pronounced double-celled Walker circulation. As will be shown later, the impact from ENSO Modoki on SEQ summer rainfall is similar to that of conventional ENSO.

Also deployed are reanalyses from the National Centers for Environmental Prediction–National Center for Atmospheric Research (NCEP–NCAR; Kalnay et al. 1996) and observed Australian rainfall since 1900 from the Australian Bureau of Meteorology. As we are interested in variability, monthly and seasonal anomalies are referenced to the climatological mean over the period 1950–2008 and are linearly detrended, unless otherwise stated.

3. Results from CMIP3 twentieth-century experiments and targeted runs

Is the summer rainfall reduction reproduced by climate models? For all but one of the experiments, the ensemble-mean trend from each model over 1950–99 is calculated (the Mk3A ozone ensemble is calculated over 1961–2000, as the model experiment starts at 1961). The uncertainty range of the trend is estimated as the standard error of the linear regression fit on the ensemble-mean data.

Several results emerge (Fig. 3). First, only four models {red crosses; Geophysical Fluid Dynamics Laboratory Climate Model version 2.1 (GFDL CM2.1), Model for Interdisciplinary Research on Climate 3.2, high-resolution version [MIROC3.2(hires)], Institute of Numerical Mathematics Coupled Model, version 3.0 (INM-CM3.0), and L'Institut Pierre-Simon Laplace Coupled Model, version 4 (IPSL CM4)} produce a rainfall decline over SEQ that is comparable to the observed. Second, the observed summer rainfall reduction is not generated in an all-model ensemble mean (orange cross), which, as an entity, contains all climate change forcing factors, such as greenhouse gases, aerosols, and stratospheric ozone depletion. Third, results from targeted experiments forced by ozone depletion only (green circle), or a comparison between the CMIP3 model groups with and without ozone depletion (orange circles), show that ozone depletion has little impact, contrary to the results from a one-model study (Syktus 2005). Finally, increasing aerosols, if anything, tend to increase SEQ summer rainfall, although the increase is very small (green crosses).

Thus, the observed rainfall decrease is not produced by the majority of models, nor is it attributable to any individual climate change forcing factor. Two possible implications may be drawn: first, climate change has little impact and much of the observed reduction is driven by internal variability; and second, climate change has an impact, but models do not capture the associated process. In either case, it is important to understand the mechanism of the observed rainfall reduction; therefore, we focus on the impact from ENSO from an observational perspective.

4. Asymmetry in ENSO and ENSO Modoki impacts

What is the impact from the ENSO cycle as an entity? ENSO can be divided into two distinct phases: El Niño and La Niña. Figure 4a depicts the relationship of SEQ austral summer rainfall with each phase through a linear fit showing a slope and a correlation using samples with positive and negative values of the indices. A distinct asymmetry emerges. A significant correlation exists during La Niña conditions, meaning that SEQ summer rainfall
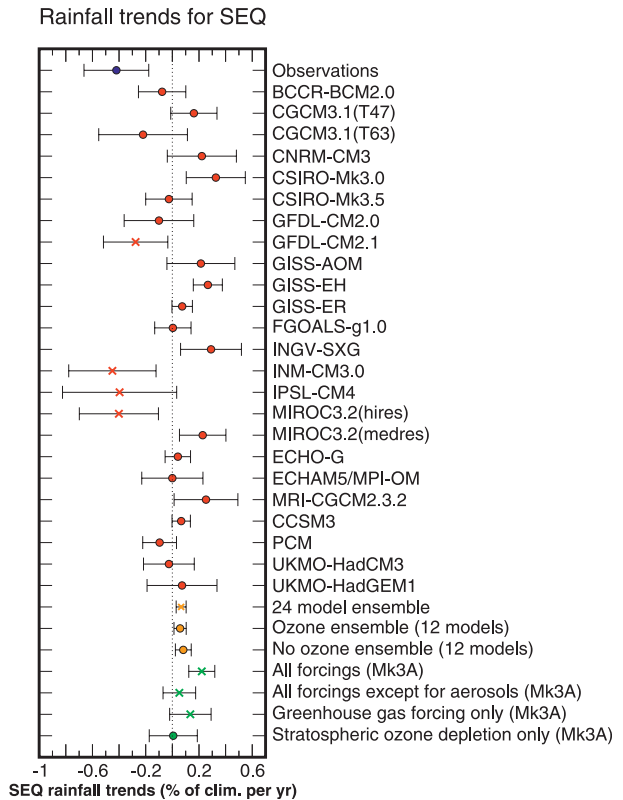
Rainfall trends for SEQ

FIG. 3. DJF rainfall trends in terms of percentage of climatology from the observed (1950–2008, blue), from IPCC twentieth-century climate model experiments (1950–99, red), and from the CSIRO Mk3A model with different forcing scenarios (green; see text for details). The error bars indicate the standard error of the linear regression of the ensemble mean.

increases as La Niña amplitude increases, with a sensitivity of approximately 109 mm °C^{-1} cooling in Niño-3.4 (a negative slope). Yet, such an ENSO–rainfall teleconnection is not evident during El Niño conditions; although rainfall tends to decrease, the influence is not statistically significant (correlation of −0.08), meaning that stronger El Niño events do not statistically generate a greater rainfall reduction. This is consistent with the findings of Power et al. (2006) for Australia-wide rainfall during June–December. The asymmetry is reproduced using the EMI (Fig. 4b), though with a higher sensitivity, suggesting that the impacts from the two types of ENSO in this season are similar. The asymmetry is also generated using an atmospheric index of ENSO [the Southern Oscillation index (SOI), see Fig. 4c] from anomalies since 1900 (Fig. 4c).

A similar analysis is conducted by regressing gridpoint circulation anomalies onto the Niño-3.4 index, using samples with negative (La Niña) and positive (El Niño) Niño-3.4 values. Maps of the associated regression coefficients (shaded) and correlation coefficients (contours)

(a) NINO3.4 & SEQ DJF Rainfall 1950-2008

s = -108.9
c = -0.43
p = 0.02

Slope (s) = -9.3
Correl. (c) = -0.08
p-value (p) = 0.68

(b) EMI & SEQ DJF Rainfall 1950-2008

s = -137.8
c = -0.34
p = 0.08

s = -30.3
c = -0.09
p = 0.62

(c) SOI & SEQ DJF Rainfall 1900-2008
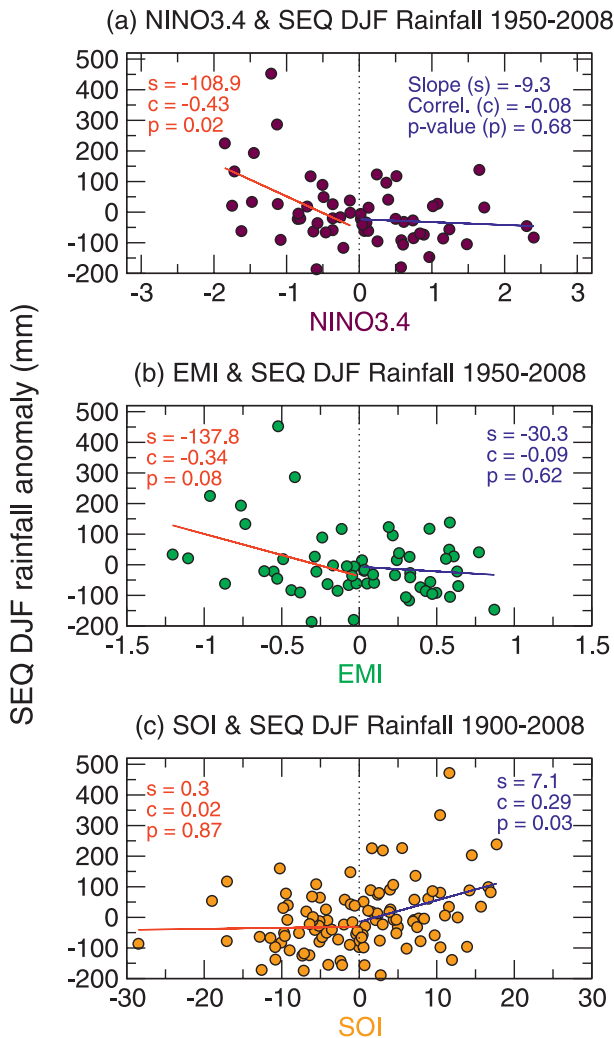
s = 0.3
c = 0.02
p = 0.87

s = 7.1
c = 0.29
p = 0.03

FIG. 4. Scatterplot of detrended SEQ DJF rainfall anomalies vs (a) detrended Niño-3.4 over the period 1950–2008, (b) detrended EMI over the period 1950–2008, and (c) detrended SOI over the period 1900–2008, with slopes, correlations, and p values of significance of the linear fits conducted separately using samples corresponding to positive and negative values of the indices.

show that during La Niña conditions (Fig. 5a) the rainfall influence is broad in scale over eastern Australia but is greatly reduced during El Niño conditions (Fig. 5d). One cause, as proposed by Power et al. (2006), could be that atmospheric circulation anomalies that lead to rainfall declines cannot reduce rainfall below zero, that is, by more than the climatological mean (~330 mm for SEQ during summer). This mechanism explains how rainfall is "capped" by El Niño events (i.e., strong events will not fall below zero), as opposed to rainfall induced by La Niña events, which is not bounded to a value. However, as the reduction in SEQ rainfall in El Niño years is generally far smaller than the amount needed to reach zero, this mechanism is unlikely to be a major contributor.

Another potential cause is the appreciable longitudinal shift in the main heating anomalies, indicating a shift in the mean convection center between La Niña and El Niño events (Hoerling et al. 1997; Cai et al. 2001; Power et al. 2006). This has been invoked to explain a nonlinear teleconnection with temperature and rainfall over North America. There is also the possibility that the forcing of the teleconnection is in itself nonlinear (Khokhlov et al. 2006), and that the nonlinearity of the ENSO cycle has become stronger in the post-1980 period (An et al. 2005). Below, we illustrate that such a zonal shift together with a difference in the response of the South Pacific convergence zone (SPCZ) is responsible for the asymmetry over SEQ.

ENSO–rainfall teleconnections are generated mainly through movements of the tropical convergence zones from their seasonal-mean positions. During La Niña, the warm pool expands meridionally and shifts westward. In association, convection reduces over the central equatorial Pacific, reflecting a westward migration of the west Pacific convergence zone, as seen in the regression/correlation between Niño-3.4 with outgoing longwave radiation (OLR, Fig. 5b). This is accompanied by an enhanced convection extending from the equatorial latitudes toward the subtropical Pacific on both sides of the equator, indicative of a poleward expansion of the intertropical convergence zone (ITCZ) and the SPCZ. In austral summer, the impact from the SPCZ is particularly important, as it reflects anomalies associated with a high-intensity warm-hemisphere convergence zone. The anomaly extends into eastern Australia, leading to an increase in rainfall over SEQ (blue, Fig. 5a). Anomalies of vertical velocities display attendant uplift motions where convection intensifies (Fig. 5c). Most importantly, the extent of the SPCZ's southward expansion and the intensity in convection are proportional to the amplitude of La Niña. This is why SEQ summer rainfall increases with La Niña amplitude.

Anomaly patterns associated with El Niño are generally similar, but maximum regression and correlation coefficients in the tropical Pacific are situated further to the east (Figs. 5e and 5f). As cooling in the west Pacific and warming in the central and eastern equatorial Pacific lead to more uniform SSTs, a merger of these major convergence zones ensues: the ITCZ and SPCZ move equatorward, and together with the convergence zone over the west Pacific, they migrate eastward, where the strongest warm SST anomalies develop. Once the merged convergence zone (i.e., the main heating region) moves sufficiently away from the west Pacific, El Niño intensity becomes irrelevant for its impacts over SEQ. Thus, the ENSO–rainfall teleconnection over SEQ is highly sensitive to an eastward shift in the mean convection center.

La Niña

(a) Rainfall

(b) OLR

(c) 500mB level vertical velocity

El Niño

(d) Rainfall

(e) OLR
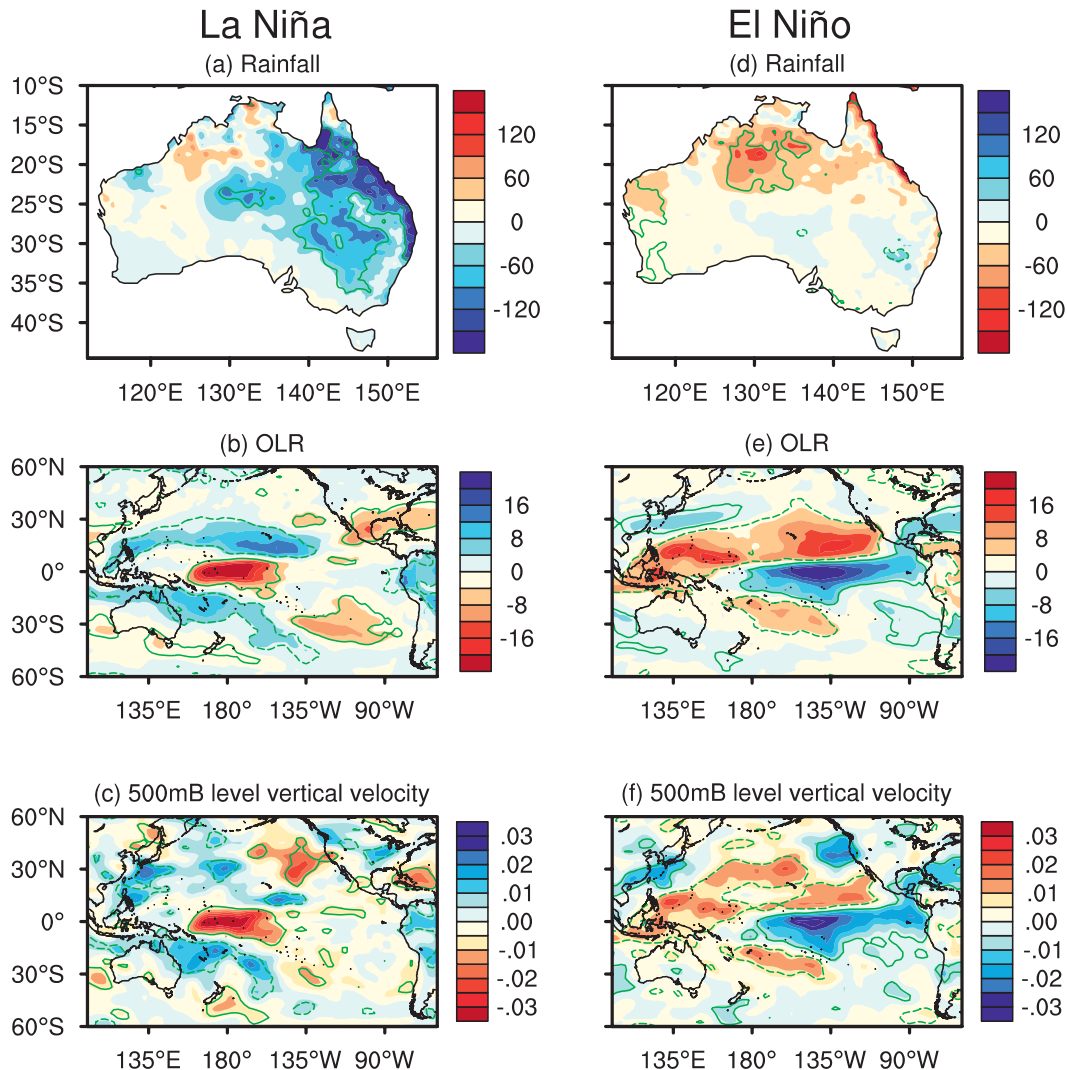
(f) 500mB level vertical velocity

FIG. 5. Anomaly patterns obtained by linearly regressing, onto negative [(left) La Niña] and positive [(right) El Niño] Niño-3.4 values (note the color reversal for ease of comparison), (a),(d) anomalies of detrended gridpoint rainfall (mm °C^{-1}), (b),(e) OLR (W m^{-2} °C^{-1}), and (c),(f) vertical velocity at 500 mb (Pa s^{-1} °C^{-1}, negative = upward motion). Dashed (solid) green contours indicate positive (negative) correlations significant at the 90% confidence level. Patterns shown are for DJF.

A similar asymmetry in circulation is generated using the EMI, as illustrated in Fig. 6. In particular, there is a strong teleconnection during La Niña Modoki phases as a result of convective heating. This is associated with a broader and stronger SPCZ that is situated over the western Pacific and intensifies with La Niña Modoki amplitudes and a weak teleconnection during El Niño Modoki phases as convergence moves sufficiently eastward.

The asymmetry means that the ENSO or ENSO Modoki cycle as an entity is conducive for SEQ summer rainfall because the rainfall increase during the La Niña years more than offsets the reduction during El Niño phases. Indeed the ENSO cycle is an important mechanism of rainfall generation for the region. Recent studies suggest that the frequency of La Niña events has been on a decline with only six events observed during 1977–2006, based on a count using the SOI, whereas the frequency of El Niño has been increasing (Power and Smith 2007). This would cause a summer rainfall reduction over SEQ, but by using Niño-3.4 and defining a La Niña as when the index amplitude exceeds a one-standard deviation value, only a slight decline in the number of La Niña events is evident throughout the past 30 yr. As we will show, since the 1980s, the ENSO–rainfall teleconnection over SEQ collapses (see Fig. 9), with La Niña or La Niña Modoki events no longer exerting a significant
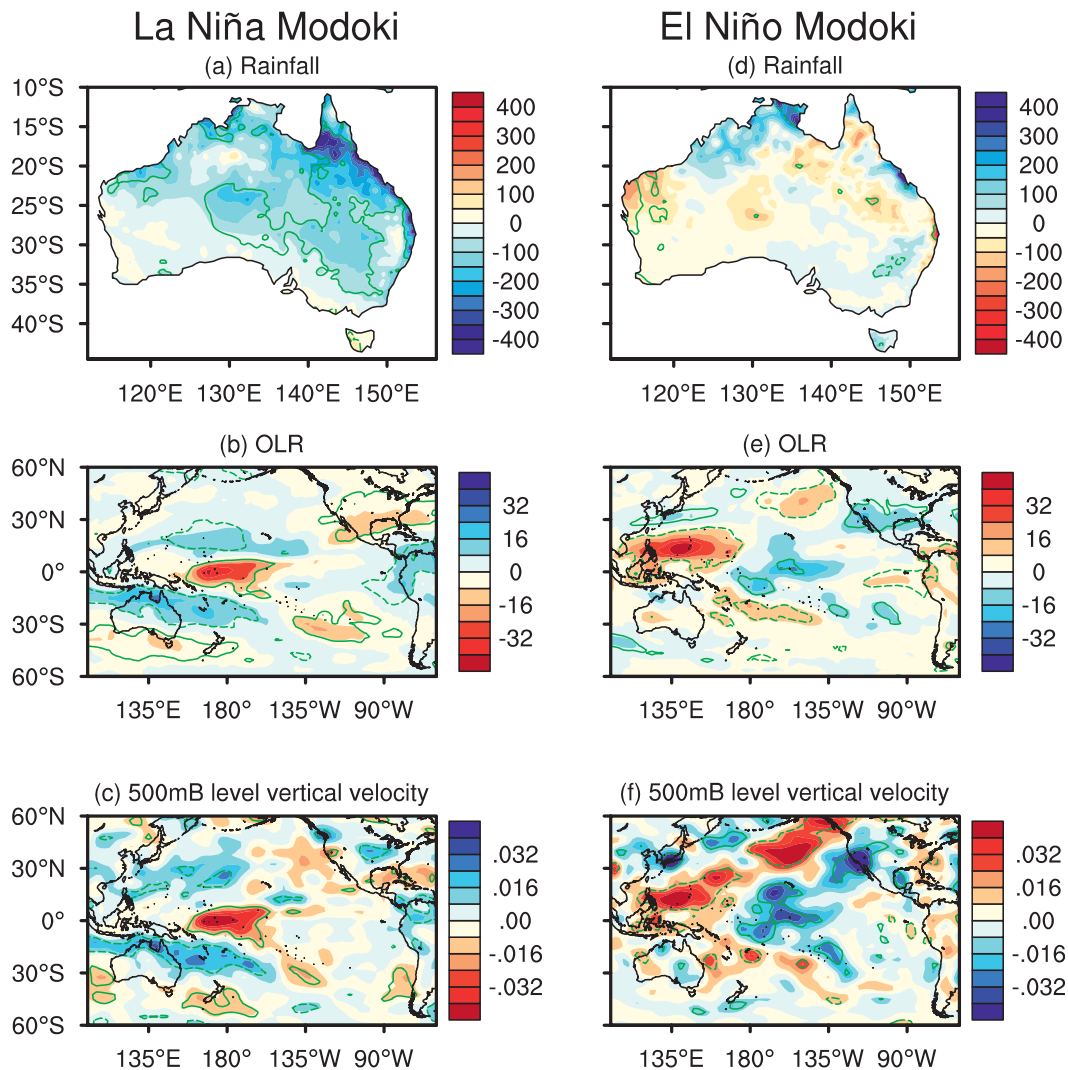
FIG. 6. As in Fig. 5, but using EMI.

influence. This appears to be the main cause behind the SEQ summer rainfall reduction.

5. A breakdown of the rainfall teleconnection since 1980

Splitting samples used in Fig. 4a into two periods, 1950–79 and 1980–2008, we see that the asymmetry within the ENSO–rainfall teleconnection is time dependent (Figs. 7a and 7d). As expected, both periods show El Niño correlations with SEQ summer rainfall that are not statistically significant. However, a very strong correlation is seen for the pre-1980 La Niña events, above the 98% confidence level, reflecting La Niña-induced strong rainfall events. [For the 90% confidence level, with 15 independent samples (13 degrees of freedom), a correlation coefficient of 0.44 is required.] By contrast, for the

post-1980 period, the impact from La Niña events is not significant, and the asymmetry between the impact of La Niña and El Niño is barely visible. Thus, the asymmetry shown in Figs. 4 and 5 predominantly exists in the pre-1980 period, with a breakdown occurring in the ENSO–rainfall teleconnection over SEQ in the post-1980 period, meaning that the summer rainfall–generating process no longer operates. This is reflected in the rainfall time series (Fig. 1b), which shows that since the 1980s there have been far fewer large seasonal totals.

Comparing the OLR regression and correlation patterns with La Niña events for the pre- and post-1980 periods (Figs. 7c and 7f), one finds that their overall patterns actually resemble each other. However, a remarkable difference exists in the warm hemisphere: the influence from the SPCZ originates from further west during the pre-1980 period than that during the post-1980 period,
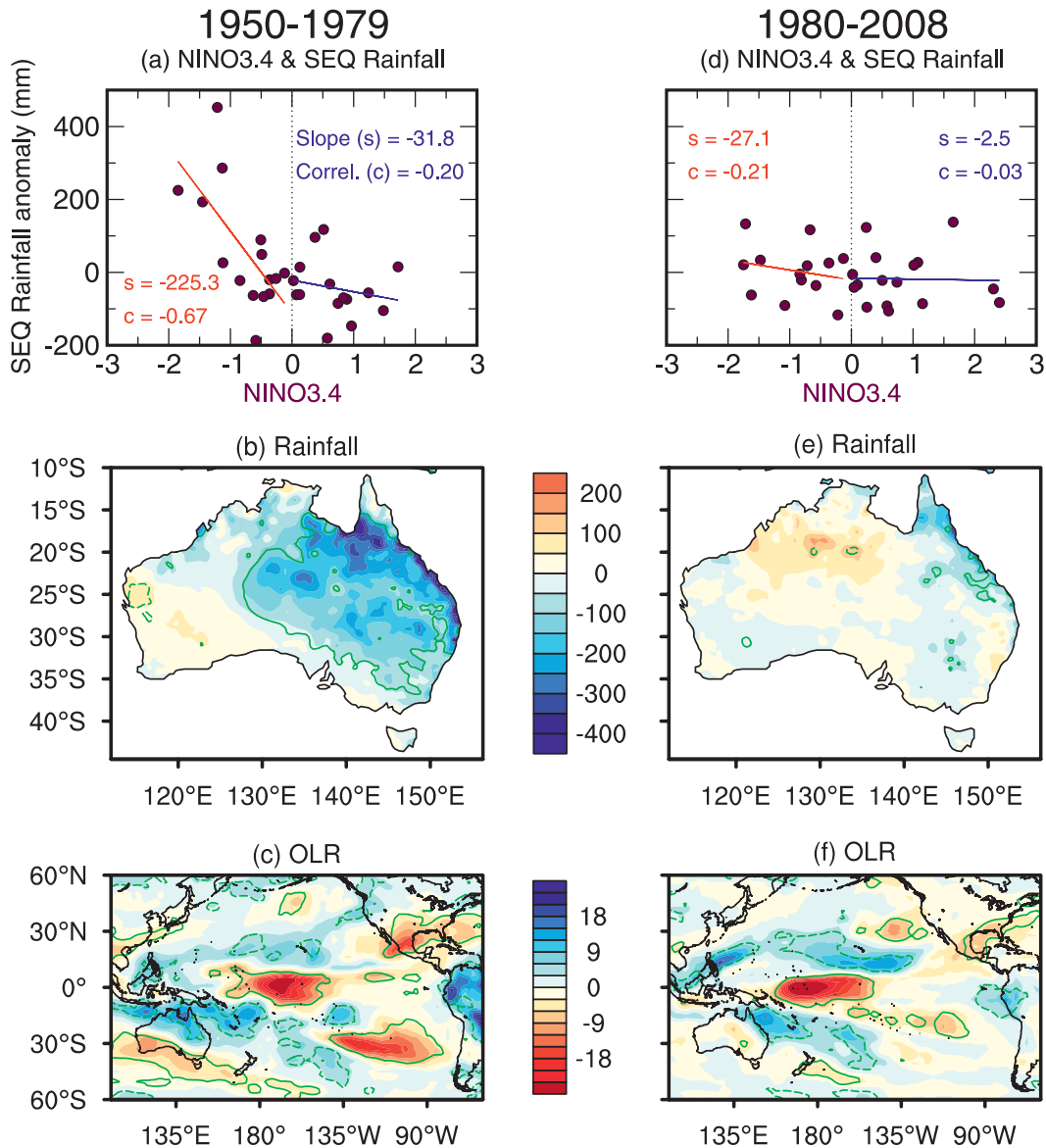
FIG. 7. (a) Scatterplot of detrended SEQ DJF rainfall anomalies vs detrended Niño-3.4, with linear fits using samples with positive and negative Niño-3.4 values, and anomaly patterns obtained by linearly regressing (b) grid-point rainfall (mm °C^{-1}) and (c) OLR (W m^{-2} °C^{-1}) onto negative Niño-3.4 values (La Niña) using corresponding samples for the period 1950–79. (d)–(f) As in (a)–(c), but for the period 1980–2008. Dashed (solid) green contours indicate positive (negative) correlations significant at the 90% confidence level.

consistent with a post-1980 eastward shift in the Walker circulation and the associated convection center. Because of the shift, despite a westward swing during La Niña events, the impact barely reaches SEQ (Figs. 7e and 7f).

The fluctuations in the asymmetry during the pre- and post-1980 periods and the associated circulation differences between the two phases generally carry over to ENSO Modoki (Fig. 8). One important feature worth noting is that SEQ summer rainfall appears to be rather

sensitive to La Niña Modoki amplitude, more so than to La Niña amplitude.

6. Multidecadal fluctuations in the teleconnection

The breakdown since 1980 is apparent in the correlations of the SEQ summer rainfall with Niño-3.4 or the EMI time series using a 13-yr sliding window (Fig. 9), showing another period of low correlation centered around 1935. Other Australian regions show similar

1950-1979

(a) EMI & SEQ Rainfall

1980-2008

(d) EMI & SEQ Rainfall

(b) Rainfall

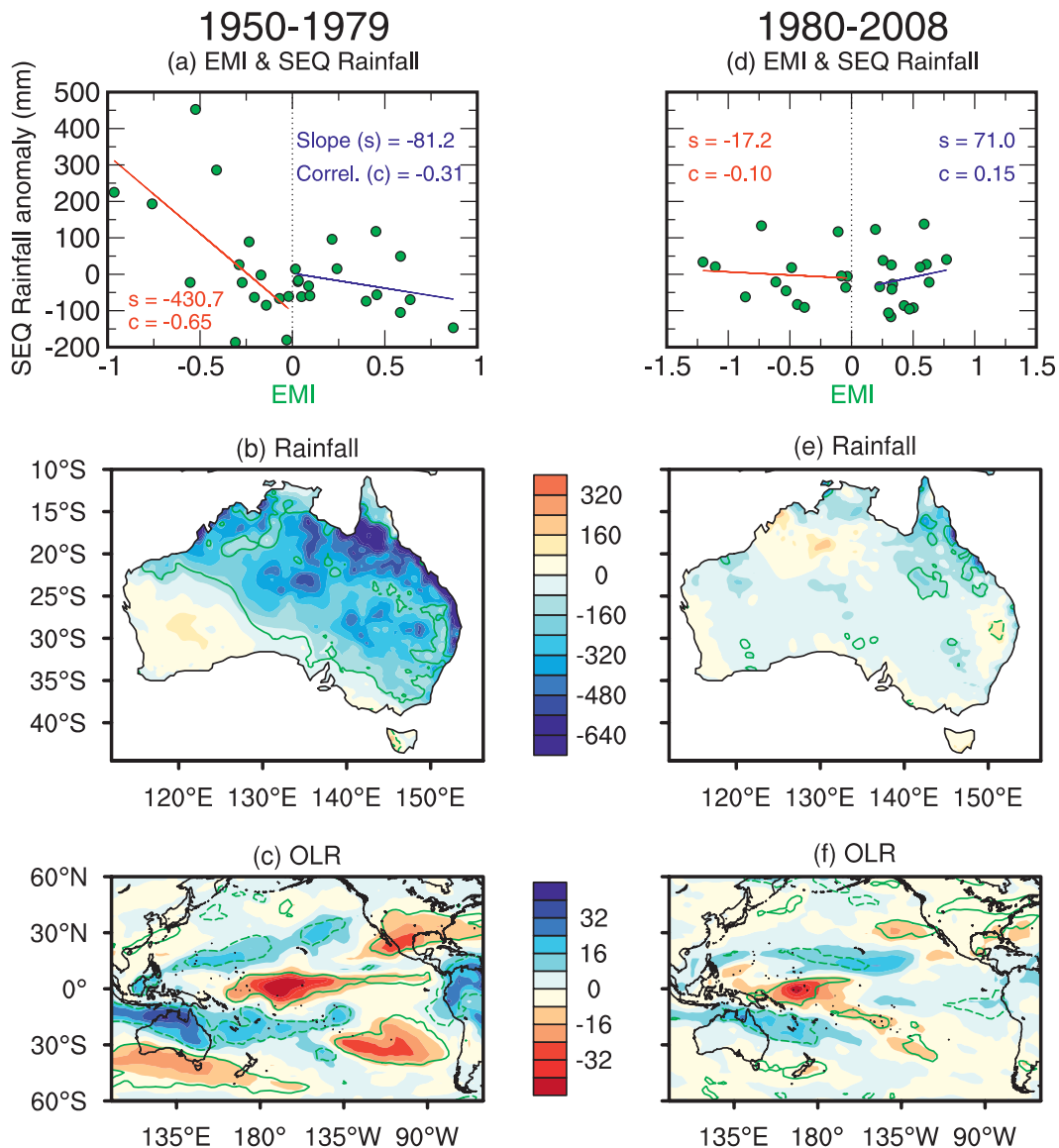### (e) Rainfall

(c) OLR

(f) OLR

FIG. 8. As in Fig. 7, but using EMI.

low rainfall correlations with ENSO during this period (Simmonds and Hope 1997). The evolution covaries with an IPO index, taken from the definition in Parker et al. (2007), similar to the correlation between ENSO and all-Australia rainfall (Power et al. 1999, 2006). During an IPO high phase, the multidecadal-mean circulations resemble those associated with El Niño. The SST anomaly pattern associated with the IPO, obtained by linear regression since 1948, features a warming in the east and a cooling in the west, though broader in scale than that associated with ENSO on an interannual basis (Figure not shown). In response, convection activities shift to the east (Fig. 10a). In association, equatorial surface easterlies, which feed into the ascending motion, decrease showing strong westerly

anomalies. These provide multidecadal-mean conditions upon which interannual ENSO or ENSO Modoki oscillate. But even during La Niña phases, when the convection center has shifted closest to Australia, the impact is small. The interannual ENSO–rainfall correlation over SEQ therefore breaks down completely, reinforcing the notion that the ENSO–rainfall teleconnection over SEQ is highly sensitive to the multidecadal-mean condition.

A similar breakdown in the influence from La Niña or La Niña Modoki occurred during the previous low-correlation period (i.e., mid-1930s; Fig. 11); likewise, there is no significant correlation during La Niña conditions nor during El Niño phases. The hypothesis that the rainfall reduction is due to the breakdown is further reinforced by the fact that
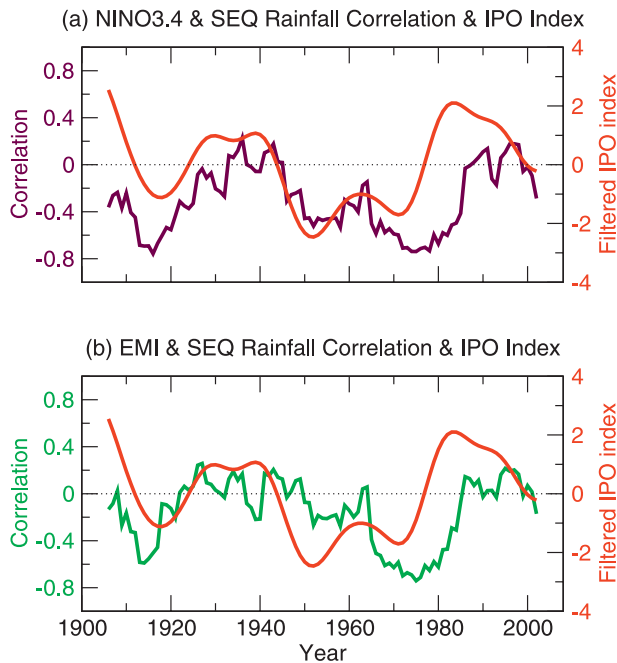
FIG. 9. Time series of correlation using a 13-yr sliding window of SEQ DJF rainfall with (a) Niño-3.4 and (b) EMI over the period 1900–2008, together with time series of an annual IPO index in red (based on the definition described by Parker et al. 2007).

FIG. 10. Anomaly pattern associated with the IPO obtained by linear regression using detrended NCEP anomalies from 1948–2007 of (a) OLR (W m^{-2} °C^{-1}) and (b) surface zonal wind (m s^{-1} °C^{-1}). Dashed (solid) green contours indicate positive (negative) correlations significant at the 90% confidence level. Patterns shown are for DJF.

there is actually an increase in the amplitude of La Niña Modoki since the 1980s, which would have induced a stronger rainfall response if the teleconnection still operated. In terms of Niño-3.4, there is no obvious trend that could explain the SEQ summer rainfall reduction either.

The fact that the breakdown in the teleconnection was also seen around 1935 suggests that multidecadal variability has the potential to generate the recent breakdown and the rainfall decline. However, this does not preclude climate change as a contributor to the breakdown and the rainfall reduction, which can usually be inferred through the use of multimodel outputs, which act to smooth out climate variability.

Figure 12 depicts a scatterplot of detrended SEQ summer rainfall anomalies versus detrended Niño-3.4 from the second half of the twentieth-century experiments based on 24 CMIP3 models for the pre- and post-1980 periods. If climate change contributes to the asymmetry and the breakdown, it should manifest in Figs. 12a and 12b, respectively, because when aggregated over such a large number of models, the contribution by multidecadal variability is largely cancelled out. As there is no asymmetry (Fig. 12a) before or after 1980, or breakdown in the post-1980 period (Fig. 12b), this suggests that climate change does not contribute to the rainfall reduction.

However, it is worth noting that most climate models suffer from a cold tongue bias in the equatorial Pacific,
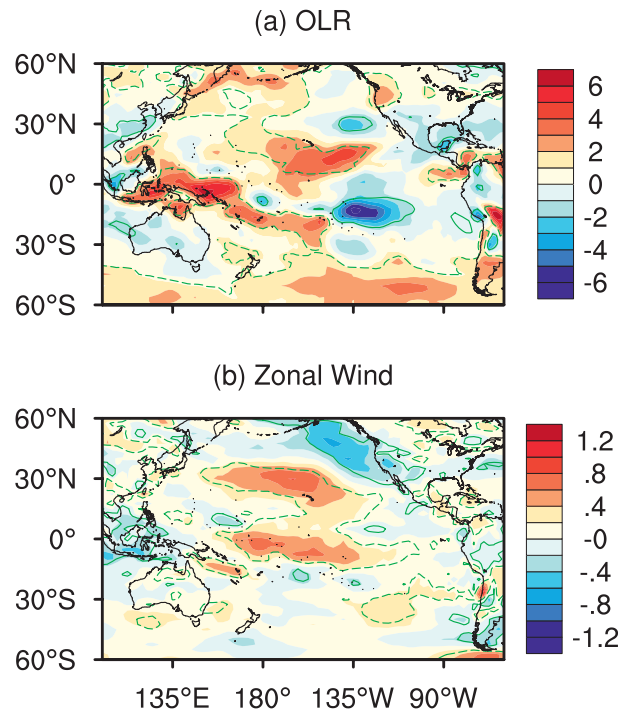
with a warm pool and the associated mean convection center located too far west (Cai et al. 2009). As a result, an unrealistic ENSO–rainfall teleconnection exists over Australia, with more models showing a significant correlation over Western Australia rather than eastern Australia (Cai et al. 2009). This means that the models' ability to simulate the different teleconnective impacts of traditional ENSO and ENSO Modoki over SEQ is also reduced. For example, only 4 out of 24 CMIP3 models produce a correlation between Niño-3.4 and SEQ summer rainfall that is comparable or greater than the observed (see Fig. 6a of Cai et al. 2009). The weaker ENSO–rainfall teleconnection over SEQ means that using these models to assess the role of climate change in the asymmetric teleconnection and its recent breakdown, and hence in the rainfall reduction, carries a fair degree of uncertainty.

7. Conclusions

We described an asymmetry in an ENSO–rainfall teleconnection and its multidecadal fluctuations. Further, the breakdown of the asymmetric nature of the teleconnection since 1980 is offered as a cause for a rainfall reduction in an ENSO-affected region of SEQ. We focus

(a) NINO3.4 & SEQ DJF Rainfall 1921-1950

Slope (s) = 9.8
Correl. (c) = 0.04
s = -37.0
c = -0.23

(b) EMI & SEQ DJF Rainfall 1921-1950
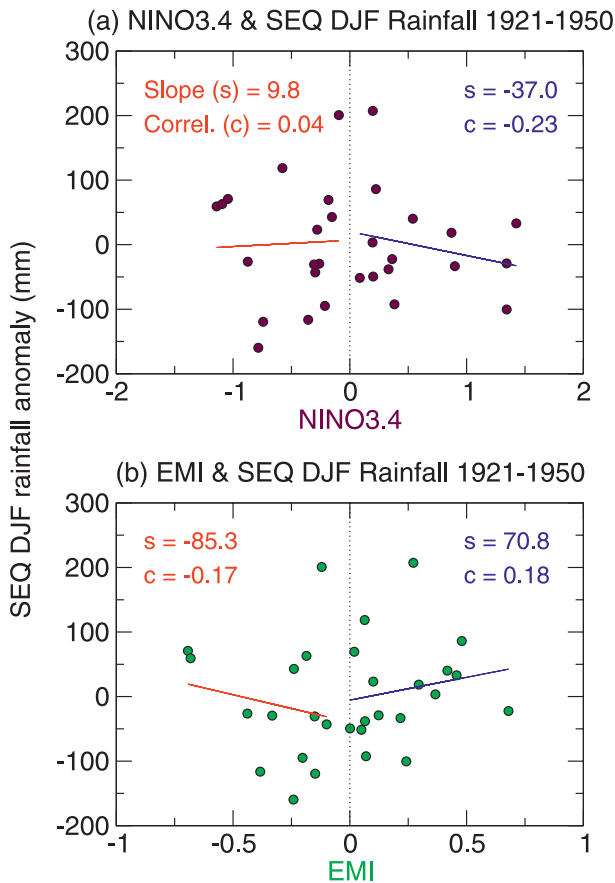
s = -85.3
c = -0.17
s = 70.8
c = 0.18

FIG. 11. Scatterplot of detrended SEQ DJF rainfall anomalies vs (a) detrended Niño-3.4, and (b) detrended EMI, with separate linear fits using samples with positive and negative values of the indices for the period 1921–50.

(a) NINO3.4 & SEQ DJF Rainfall 1950-1979

Slope (s) = -15.5
Correl. (c) = -0.13
s = -16.7
c = -0.14

(b) NINO3.4 & SEQ DJF Rainfall 1980-1999

s = -25.3
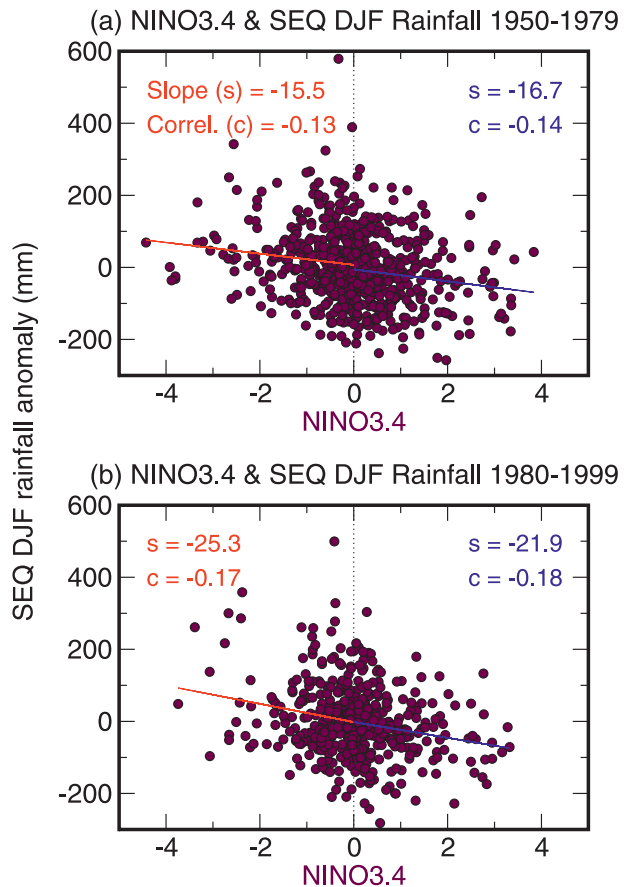c = -0.17
s = -21.9
c = -0.18

FIG. 12. Scatterplot of detrended SEQ DJF rainfall anomalies vs detrended Niño-3.4 from the second half of the twentieth-century experiments based on 24 CMIP3 models (a) for the pre-1980 (1950–79) and (b) post-1980 period (1980–99). Separate linear fits using samples with positive and negative values of the index are also shown.

on what drives the observed SEQ summer rainfall decline since the 1980s. We show that the decline is not simulated by the majority of climate models forced with anthropogenic forcing factors, such as greenhouse gases, ozone depletion, or aerosols. We therefore examine climate variability as a possible driver and show that the impact of ENSO on SEQ summer rainfall is nonlinear: La Niña events induce a statistically significant rainfall increase, but El Niño events do not generate a statistically significant reduction. Since 1980, there is a breakdown in the teleconnection with La Niña over the region, such that La Niñas no longer bring strong rainfall events, contributing to the reduction.

Such an asymmetry undergoes multidecadal fluctuations and is sensitive to the multidecadal-mean position of the tropical Pacific main convection center, particularly the SPCZ during austral summer. Since 1980, associated with the positive phase of the IPO, an eastward shift occurs in the Walker circulation and the associated convection center. As a consequence of this multidecadal-long

eastward shift, even with a La Niña-induced movement to the west, the convection center responsible for SEQ rainfall barely makes an imprint in the SEQ region, contributing to the reduction.

A similar asymmetry and a post-1980 breakdown exist in the impact from ENSO Modoki. The asymmetry suggests that ENSO Modoki as an entity is similarly rain conducive for the region. The resemblance to the traditional ENSO arises because in this season there is little difference in the circulation anomalies between the two types of ENSO.

Early in the twentieth century, when the IPO was in another positive phase, a similar breakdown was seen, indicating that multidecadal variability has the potential to cause the recent decline. However, this may not exclude a coimpact from climate change. Aggregated over the 24 CMIP3 twentieth-century experiments used in this study, there is no asymmetry in the ENSO–rainfall teleconnection over the period of 1950–79, or a breakdown

in the post-1980 period (1980–99), suggesting that climate change may not be a forcing. However, because the majority of climate models do not perform well in simulating the observed ENSO–rainfall teleconnection over the SEQ region, the robustness of this result needs to be further tested. It is therefore essential for models to realistically simulate this teleconnection before they are used in attribution studies in ENSO-affected regions.

REFERENCES

Alexander, L. V., P. Hope, D. Collins, B. Trewin, A. Lynch, and N. Nicholls, 2007: Trends in Australia's climate means and extremes: A global context. *Aust. Meteor. Mag.,* **56,** 1–18.

An, S.-I., W. W. Hsieh, and F.-F. Jin, 2005: A nonlinear analysis of the ENSO cycle and its interdecadal changes. *J. Climate,* **18,** 3229–3239.

Ashok, K., S. K. Behera, S. A. Rao, H. Weng, and T. Yamagata, 2007: El Niño Modoki and its possible teleconnection. *J. Geophys. Res.,* **112,** C11007, doi:10.1029/2006JC003798.

Cai, W., and T. Cowan, 2006: SAM and regional rainfall in IPCC AR4 models: Can anthropogenic forcing account for southwest Western Australian winter rainfall reduction? *Geophys. Res. Lett.,* **33,** L24708, doi:10.1029/2006GL028037.

——, and ——, 2008: Dynamics of late autumn rainfall reduction over southeastern Australia. *Geophys. Res. Lett.,* **35,** L09708, doi:10.1029/2008GL033727.

——, and ——, 2009: La Niña Modoki impacts Australia autumn rainfall variability. *Geophys. Res. Lett.,* **36,** L12805, doi:10.1029/2009GL037885.

——, P. H. Whetton, and A. B. Pittock, 2001: Fluctuations of the relationship between ENSO and northeast Australian rainfall. *Climate Dyn.,* **17,** 421–432.

——, G. Shi, and Y. Li, 2005: Multidecadal fluctuations of winter rainfall over southwest Western Australia simulated in the CSIRO mark 3 coupled model. *Geophys. Res. Lett.,* **32,** L12701, doi:10.1029/2005GL022712.

——, A. Sullivan, and T. Cowan, 2009: Rainfall teleconnections with Indo-Pacific variability in the WCRP CMIP3 models. *J. Climate,* **22,** 5046–5071.

Collins, M., 2005: El Niño- or La Niña-like climate change? *Climate Dyn.,* **24,** 89–104.

Hoerling, M. P., A. Kumar, and M. Zhong, 1997: El Niño, La Niña, and the nonlinearity of their teleconnections. *J. Climate,* **10,** 1769–1786.

Hope, P., W. Drosdowsky, and N. Nicholls, 2006: Shifts in the synoptic systems affecting southwest Western Australia. *Climate Dyn.,* **26,** 751–764.

Kalnay, E., and Coauthors, 1996: The NCEP/NCAR 40-Year Reanalysis Project. *Bull. Amer. Meteor. Soc.,* **77,** 437–471.

Khokhlov, V. N., A. V. Glushkov, and N. S. Loboda, 2006: On the nonlinear interaction between global teleconnection patterns. *Quart. J. Roy. Meteor. Soc.,* **132,** 447–465.

McBride, J. L., and N. Nicholls, 1983: Seasonal relationships between Australian rainfall and the Southern Oscillation. *Mon. Wea. Rev.,* **111,** 1998–2004.

Meehl, G. A., and W. Washington, 1996: El Niño-like climate change in a model with increased atmospheric CO_2 concentrations. *Nature,* **382,** 56–60.

——, A. Hu, and B. D. Santer, 2009: The mid-1970s climate shift in the Pacific and the relative roles of forced versus inherent decadal variability. *J. Climate,* **22,** 780–792.

Parker, D., C. Folland, A. Scaife, J. Knight, A. Colman, P. Baines, and B. Dong, 2007: Decadal to multidecadal variability and the climate change background. *J. Geophys. Res.,* **112,** D18115, doi:10.1029/2007JD008411.

Philander, S. G., 1990: *El Niño, La Niña, and the Southern Oscillation.* Academic Press, 289 pp.

Power, S. B., and I. N. Smith, 2007: Weakening of the Walker Circulation and apparent dominance of El Niño both reach record levels, but has ENSO really changed? *Geophys. Res. Lett.,* **34,** L18702, doi:10.1029/2007GL030854.

——, T. Casey, C. Folland, A. Colman, and V. Mehta, 1999: Interdecadal modulation of the impact of ENSO on Australia. *Climate Dyn.,* **15,** 319–324.

——, M. Haylock, R. Colman, and X. Wang, 2006: The predictability of interdecadal changes in ENSO activity and ENSO teleconnections. *J. Climate,* **19,** 4755–4771.

Rayner, N. A., D. E. Parker, E. B. Horton, C. K. Folland, L. V. Alexander, D. P. Rowell, E. C. Kent, and A. Kaplan, 2003: Global analyses of sea surface temperature, sea ice, and night marine air temperature since the late nineteenth century. *J. Geophys. Res.,* **108,** 4407, doi:10.1029/2002JD002670.

Ropelewski, C. F., and M. S. Halpert, 1987: Global and regional scale precipitation patterns associated with El Niño–Southern Oscillation. *Mon. Wea. Rev.,* **115,** 1606–1626.

Rotstayn, L. D., and Coauthors, 2007: Have Australian rainfall and cloudiness increased due to the remote effects of the Asian anthropogenic aerosols? *J. Geophys. Res.,* **112,** D09202, doi:10.1029/2006JD007712.

Simmonds, I., and P. Hope, 1997: Persistence characteristics of Australian rainfall anomalies. *Int. J. Climatol.,* **17,** 597–613.

Smith, I. N., P. McIntosh, T. J. Ansell, C. J. C. Reason, and K. L. McInnes, 2000: Southwest Western Australian winter rainfall and its association with Indian Ocean climate variability. *Int. J. Climatol.,* **20,** 1913–1930.

Syktus, J., 2005: Reasons for decline in eastern Australia's rainfall. *Bull. Amer. Meteor. Soc.,* **86,** 624.

Vecchi, G. A., B. J. Soden, A. T. Wittenberg, I. M. Held, A. Leetmaa, and M. J. Harrison, 2006: Weakening of tropical Pacific atmospheric circulation due to anthropogenic forcing. *Nature,* **441,** 73–76.

Wang, B., 1995: Interdecadal changes in El Niño onset in the last four decades. *J. Climate,* **8,** 267–285.

Wang, G., and H. H. Hendon, 2007: Sensitivity of Australian rainfall to inter-El Niño variations. *J. Climate,* **20,** 4211–4226.